J. Am. Soc. Mass Spectrom. (2017) 28:901–907
DOI: 10.1007/s13361-017-1610-6

RESEARCH ARTICLE

Potential of *Burkholderia seminalis* TC3.4.2R3 as Biocontrol Agent Against *Fusarium oxysporum* Evaluated by Mass Spectrometry Imaging

Francisca Diana da Silva Araújo,[1] Welington Luiz Araújo,[2] Marcos Nogueira Eberlin[1]

[1]ThoMSon Mass Spectrometry Laboratory, Institute of Chemistry, University of Campinas, UNICAMP, 13083-970, Campinas, SP, Brazil
[2]Department of Microbiology, Institute of Biomedical Sciences, University of São Paulo, USP, São Paulo, 05508-900, SP, Brazil

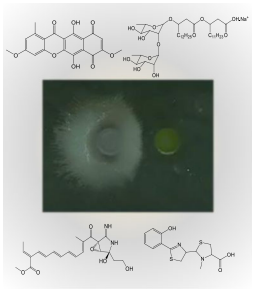

Abstract. Species of genus *Burkholderia* display different interaction profiles in the environment, causing either several diseases in plants and animals or being beneficial to some plants, promoting their growth, and suppressing phytopathogens. *Burkholderia* spp. also produce many types of biomolecules with antimicrobial activity, which may be commercially used to protect crops of economic interest, mainly against fungal diseases. Herein we have applied matrix-assisted laser desorption/ionization mass spectrometry imaging (MALDI-MSI) to investigate secondary metabolites produced by *B. seminalis* TC3.4.2R3 in monoculture and coculture with plant pathogen *Fusarium oxysporum*. The siderophore pyochelin and the rhamnolipid Rha-Rha-C15-C14 were detected in wild-type *B. seminalis* strain, and their productions were found to vary in mutant strains carrying disruptions in gene clusters associated with antimicrobial compounds. Two mycotoxins were detected in *F. oxysporum*. During coculture with *B. seminalis*, metabolites probably related to defense mechanisms of these microorganisms were observed in the interspecies interaction zone. Our findings demonstrate the effective application of MALDI-MSI in the detection of bioactive molecules involved in the defense mechanism of *B. seminalis*, and these findings suggest the potential use of this bacterium in the biocontrol of plant diseases caused by *F. oxysporum*.

Keywords: Mass spectrometry imaging, *Burkholderia seminalis*, *Fusarium oxysporum*

Received: 17 October 2016/Revised: 18 January 2017/Accepted: 19 January 2017/Published Online: 13 February 2017

Introduction

Current insights into microbial interactions in the environment have emerged from model studies with crop plant species, based on the species abundance and functional metagenomics. However, over the past years, the molecular features related to microbial interactions have attracted interest, allowing the identification of new molecules related to microbial interaction and also the use in applied sciences [1]. Rhizosphere microorganisms are ideal as biocontrol agents for providing a front line defense for roots against pathogen attack [2, 3]. This defense can occur through several mechanisms such as competition for nutrients, parasitism, induced systemic resistance, or the release of biologically active secondary metabolites (antibiosis) [4].

Species of *Burkholderia* spp. have shown great potential in disease suppression and bioremediation by antimicrobial metabolite production [5–7]. The antagonism of *Burkholderia* spp. mainly against phytopathogenic fungi and oomycetes is well established [8–11], and several secondary metabolites have been characterized such as pyrrolnitrin [12], phenazines [13], cepacidines [14], lipopeptides [15], rhamnolipids [16], cepaciamides A and B [17], siderophores [18], glidobactins [19, 20], altericidin [21], and 2-hydroxymethyl-chroman-4-one [22].

The *B. seminalis* strain TC3.4.2R3 has been isolated from the surface of disinfected sugarcane roots, and was found to present antagonism against plant pathogens *Fusarium verticiloides* and *Xanthomonas albilineans* [23], and to suppress orchid necrosis caused by *Burkholderia gladioli* [7]. Although some genes related to this interaction have been identified [7], the metabolites involved in this microbial

Electronic supplementary material The online version of this article (doi:10.1007/s13361-017-1610-6) contains supplementary material, which is available to authorized users.

Correspondence to: Francisca Diana da Silva Araújo;
e-mail: fdsaraujo@gmail.com

interaction have remained unknown. Recently, matrix-assisted laser desorption/ionization mass spectrometry imaging (MALDI-MSI) has been introduced as an efficient tool to screen the 2D spatial distribution of biomolecules involved in metabolic exchanges during microbial interactions [24–26]. Such chemically selective imaging has led to advanced understanding of the chemical signaling processes, allowing simultaneous detection and spatial monitoring of multiple metabolites. *F. oxysporum* is a fungus that causes diseases in several crops of major agricultural interest such as bean, sugarcane [27], and banana [28]. Herein we have applied MALDI-MSI to spatially monitor and characterize secondary metabolites produced by *B. seminalis* TC3.4.2R3 in monocultures and cocultures with *F. oxysporum*.

Experimental

Strains and Materials

The sugarcane root endophyte *B. seminalis* TC3.4.2R3 and the phytopathogen *F. oxysporum* were obtained from *Saccharum officinarum* and maintained in culture medium PDA (potato dextrose agar, Difco). The TC3.4.2R3 mutants present a TN5 transposon inserted in the *wcbE* gene, which encode a glycosyltransferase [7].

The α-cyano-4-hydroxy-cinnamic acid (CHCA, 99%), trifluoroacetic acid (TFA, 99%), acetonitrile (≥99.9%), and methanol (≥99.9%) HPLC grade were purchased from Sigma-Aldrich (Steinheim, Germany), conductive indium tin oxide (ITO)-coated glass slides and peptide calibration standard II from Bruker Daltonics (Bremen, Germany).

Monoculture and Coculture of Microorganisms

Conductive indium tin oxide (ITO)-coated glass slides were placed in a sterile Petri dish and deposited a thin film 0.5–1.0 mm of PDA medium (approximately 10 mL). On this plate, 0.5 μL of cell suspension of wild-type *B. seminalis* strain, suspended in sterile water (1:1, m/v), was applied. After incubation, the MALDI glass slide was removed from the Petri dish and dehydrated in a desiccator under vacuum. The matrix CHCA was prepared using 50% acetonitrile:water in 2.5% trifluoroacetic acid, and then it was manually sprayed on the slide using a glass sprinkler. An optical image was taken of the slide before and after the matrix application. The slide was supported in a MTP slide-adapter II (Bruker Daltonics, Bremen, Germany) and the target loaded into the MALDI-TOF spectrometer (Supplementary Scheme S1). Wild and mutant *B. seminalis* strains were analyzed by MALDI-MSI in growth times of 24, 48, and 72 h. The MALDI glass slides of *F. oxysporum* were prepared similarly and examined by MALDI-MSI at 30 h of incubation. For coculture experiments, cell suspension of *B. seminalis* was applied at 5 mm distance from a *F. oxysporum* inoculum on MALDI glass slides containing PDA medium placed in Petri dishes, inoculated in biochemical oxygen demand (B.O.D.) incubator at 30 °C for 30 h. Similar experiments were developed with mutants and the fungus, and analyzed by MALDI-MSI (Supplementary Scheme S1) [24].

MALDI-MSI Conditions

Slides containing the microorganisms were submitted to MSI in the Autoflex Bruker Daltonics TOF mass spectrometer in the positive ion reflector mode, with 200 μm laser intervals in XY, controlled by FlexControl 3.3 software package (Bruker Daltonics) using the RP_pepMix.par method. Data were acquired in the AutoXecute command with accumulation in parent mode on, and sum up to 600 satisfactory shots in 600 shots. Laser power was adjusted to 50% and voltage of the ion source 1, ion source 2, lens, reflector 1, and reflector 2 were set to 20.00, 17.47, 8.80, 22.00, and 10.10 kV, respectively. The pulsed ion extraction time was 30 ns, the suppression mass gate was set to *m/z* 100, and the detector gain was 7. The processing method used was FC_PepMix, which corresponds to a parameter set to pick picking, smoothing, and baseline subtract. The calibration of the equipment was performed using peptide calibration standard II and matrix ions. All MSI experiments were performed in triplicate.

MALDI-MSI Data Processing

After acquisitions, datasets were analyzed by FlexImaging. The resulting mass spectrum was filtered manually in 0.5–1.0 Da increments by selecting ions of interest from the average spectrum or from individual spectra, with individual colors assigned to the specific masses. The spectra were internally calibrated by matrix ions, and the images normalized using the TIC mode.

Data Analysis Using SCiLS Lab

Image datasets were also analyzed using the software SCiLS Lab (SCiLS GmbH, Bremen, Germany). The dataset was used with minimal *m/z* value of 150–850 Da and interval width of ±0.2 Da, and submitted to the baseline removal, normalization regarding total ion count (TIC), and peak alignment. The datasets of wild-type *B. seminalis* and mutant strains were compared by principal component analysis (PCA) applied to the individual spectra [29].

Identification of Interest Compounds

For identification of ions detected by MALDI-MSI, MS/MS data were obtained by direct analysis of the cells by MALDI-MS/MS, or from extracts of each microorganism by electrospray ionization coupled with Fourier-transform ion cyclotron resonance mass spectrometry (ESI-FT-ICR-MS, Thermo Fisher Scientific Inc., Bremen, Germany) or electrospray ionization coupled with quadrupole time-of-flight mass spectrometry (ESI-Q-TOF-MS, Agilent Technologies Inc., Santa Clara, CA, USA). For MALDI-MS/MS analysis, *B. seminalis* (wild-type and mutants) and *F. oxysporum* strains were grown on PDA medium, in a B.O.D. incubator at 30 °C and 24 h.

After this time, the microorganism cells were suspended in sterile water (1:1, m/v). The suspensions (5 μL) of each microorganism were diluted in 100 μL sterile water and spotted (1 μL) onto a steel target plate (MSP 96 polished-steel target; Bruker Daltonics, Bremen, Germany), allowed to dry at room temperature, and covered with the matrix solution (1 μL), which consisted of CHCA dissolved in 50% acetonitrile and 2.5% trifluoroacetic acid. Subsequently, the droplet was completely evaporated and the target loaded into the MALDI-TOF mass spectrometer. For ESI-FT-ICR-MS or ESI-Q-TOF-MS analyses, the extracts were prepared via cultivation of each microorganism on PDA medium, and small pieces of agar were extracted with H_2O:acetonitrile:TFA (50:50:2.5). ESI-FT-ICR-MS conditions: MS and MS/MS spectra were acquired in a LTQ FT Ultra 7 T mass spectrometer by direct infusion operating at a flow rate of 10 μl min^{-1}, source voltage of 3.64 kV, capillary temperature of 280 °C, and capillary and tube lens voltages of 47.97 V and 134.73 V, respectively. The ions of interest were isolated by linear ion trap and fragmented by collision induced dissociation (CID) using collision energy at 15–45 eV. The data were acquired and processed using Xcalibur 3.0.63 software. ESI-Q-TOF-MS conditions: a 6550 iFunnel Q-TOF LC/MS mass spectrometer was used by flow injection analysis with injection volume of 5 μL, flow rate of 0.4 mL min^{-1}, and elution with 50% of solvent B (solvent A = water containing 0.1% of formic acid; solvent B = acetonitrile). The capillary voltage was set at 3000 V, nozzle voltage of 320 V, gas temperature of 290 °C, pressure of nebulizer gas of 45 psig, sheath gas of 12 L min^{-1} and 350 °C, voltages of Fragmentor and Octopole 1 rf $V_{p\text{-}p}$ were 100 and 750 V, respectively. Collision energy was used at 15–45 eV for fragmentation. The accurate *m/z* and fragmentation patterns were compared with those reported in databases, such as MassBank and METLIN, as well as in previous reports.

Results and Discussion

To determine spatial and temporal distributions of the secreted metabolites, wild-type *B. seminalis* TC3.4.2R3 colonies were submitted to MALDI-MSI after 24, 48, and 72 h of incubation. After 24 h, many metabolites produced by the bacterium were detected by MALDI-MSI (Supplementary Figure S1), and the colony-localized ones could be differentiated from the diffusible metabolites. Diffusible metabolites are of special interest since they may have an important role in the antimicrobial activity. Larger spatial distributions of diffuse metabolites were observed as a function of incubation time. To better characterize these metabolites, a *B. seminalis* extract was analyzed by a high accuracy and high resolution mass spectrometer, that is, via ESI-FT-ICR-MS. For the ion of nominal *m/z* 325, the accurate *m/z* 325.0672 (Supplementary Figure S2) determined for the protonated molecule, as well as its dissociation pattern accessed via ESI-FT-ICR-MS/MS experiments, permitted its identification as pyochelin (Δ = –1.2 ppm; Figure 1a and Supplementary Figure S3). This molecule is a known siderophore also found in the bacterium *P. aeruginosa,* and it may promote the virulence of *B. seminalis*, since pyochelin plays a central role in iron sequestration [25, 30]. The gene cluster for this siderophore was already identified in the *B. seminalis* TC3.4.2R3 genome [7]. For *m/z* 799, its accurate *m/z* 799.5186 (Supplementary Figure S2) and the dissociation pattern of its sodiated molecule $[M + Na]^+$ pointed to L-rhamnosyl-L-rhamnosyl-3-hydroxypentadecanoyl-3-hydroxytetradecanoate (Rha-Rha-C15-C14) (Δ = 1.0 ppm; Figure 1a and Supplementary Figure S4). Based on the chemistry of analogous molecules [31–33], the ESI-FT-ICR-MS/MS of the sodiated rhamnolipid display fragment ions of *m/z* 653 likely due to the loss of rhamnose residue, *m/z* 169 assigned to the rhamnose residue $[Rha_{res} + Na]^+$, *m/z* 187 due to the loss of a rhamnose unit $[Rha + Na]^+$, and *m/z* 559 due to the loss of the terminal fatty acid chain. The production of Rha-Rha-C15-C14 by *B. seminalis* was also corroborated by the detection by ESI-FT-ICR-MS of the $[M + K]^+$ ion of *m/z* 815.4926 (Δ = 1.0 ppm). In addition, genome analysis of this TC3.4.2R3 strain [7] has also show a gene (Bsem_06536-06543) associated with its production. Rhamnolipids, such as Rha-Rha-C15-C14, have also been found in *B. pseudomallei* showing cytotoxic and hemolytic activities [33], and in *Burkholderia thailandensis* [31], but are mainly produced by *Pseudomonas aeruginosa*, in which they facilitate surface motility and affect biofilm architecture contributing to survival in diverse environments [34–36]. The colony-localized ion of *m/z* 714 was characterized by the MALDI-MS/MS and attributed to polyglutamate (Figure 1a and Supplementary Figure S5), which is known to be a marker for extracellular matrix previously found in *Bacillus subtilis* [24], *P. aeruginosa*, and *B. pumilus* [37].

Cultures of strains carrying disruptions in the gene *wcbE* were also subjected to MALDI-MSI. This gene encodes a glycosyltransferase, and mutants have been found to lose the ability to suppress orchid necrosis caused by *B. gladioli* [7] and inhibit the fungus *F. oxysporum* [38]. The software SCiLS Lab (SCiLS GmbH) was used to compare and evaluate the MALDI-MSI datasets by chemometric analysis [29]. The PCA of all individual spectra was able to separate the wild-type *B. seminalis* strain TC3.4.2R3 (blue) from the mutant strains at 24 h of incubation time (Figure 1b). But at longer incubation times (48 h and 72 h), the PCA separation efficiency diminishes. After 24 h of incubation, the diffuse metabolites detected for the wild-type *B. seminalis* (*m/z* 247, 275, 277, 279, and 325 in Supplementary Figure S1) were absent for almost all mutants (M3, M4, and M7), confirming the involvement of such diffuse metabolites in the inhibitory activity of *B. seminalis*. Later (48 h and more at 72 h), however, these diffuse metabolites are again detected at lower abundances (see, for instance, the detection of pyochelin in Figure 1c), demonstrating that their productions have not been fully silenced but only delayed. Interestingly, the productions of almost all colony-associated ions in the mutants remained the same compared with wild-type strain (see polyglutamate in Figure 1a, and all ions in Supplementary Figure S1), except the rhamnolipid (*m/z* 799), which seems to

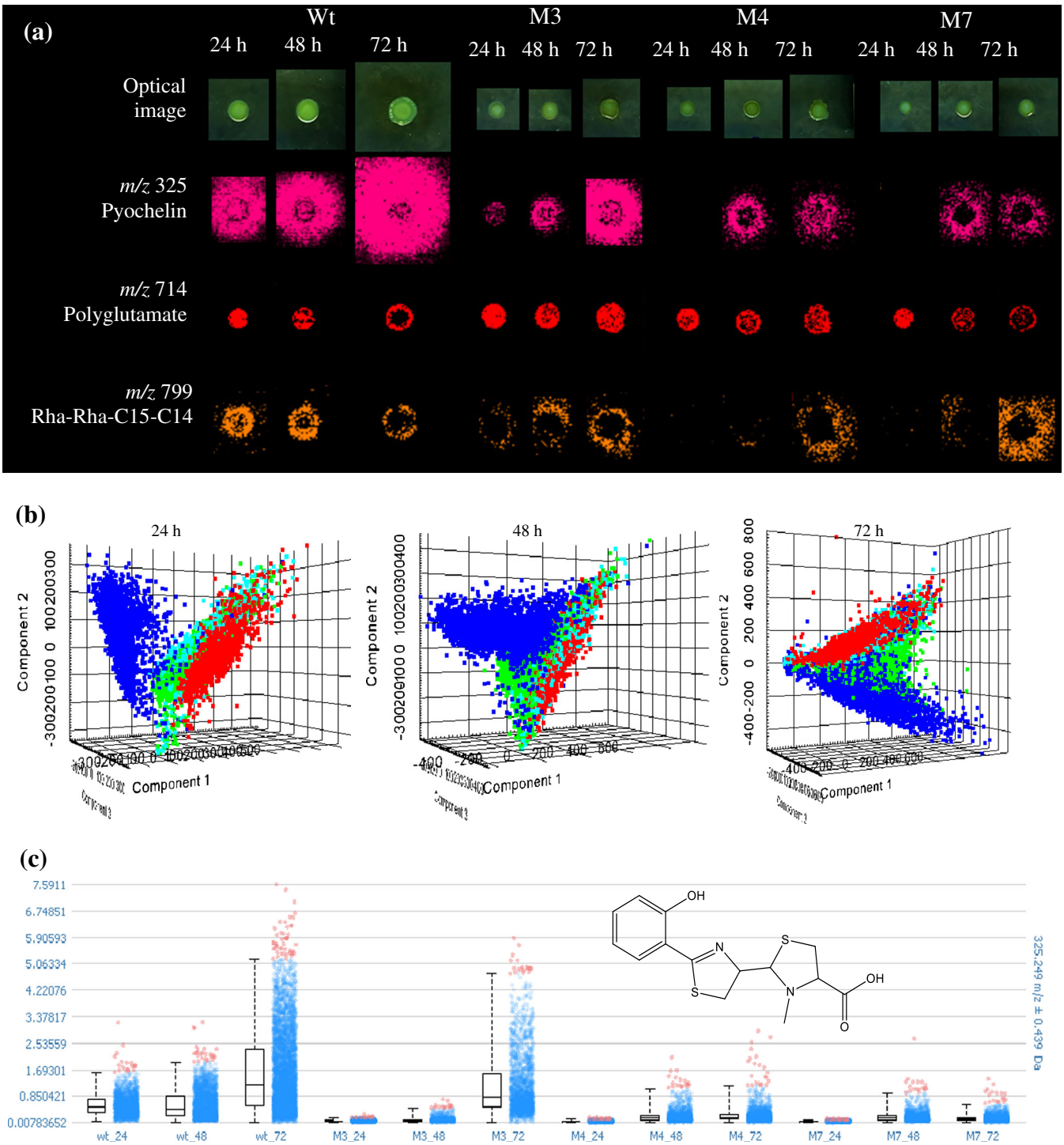

Figure 1. **(a)** MALDI-MSI of *B. seminalis* metabolites in incubation times of 24, 48, and 72 h on PDA medium. **(b)** Comparison among wild-type *B. seminalis* (blue) and M3 (red), M4 (green), and M7 (light blue) mutant strains by PCA of the individual spectra of each image obtained. **(c)** Box plot of the ion abundances (*m/z* 325) of pyochelin. Wt: wild-type *B. seminalis*; M3/M4/M7 = *B. seminalis* mutants

be altered in the mutants (Figure 1a). Rhamnolipids are synthesized through sequential glycosyltransferase reactions comprising two distinct rhamnosyltransferase enzymes [39]. Although the gene cluster for rhamonolipids was annotated in the *B. seminalis* TC3.4.2R3, the present result suggests that this glycosyltransferase, of which the related gene is also present in another cluster and which was knockout in the mutant, may participate in the synthesis of this rhamnolipid.

F. oxysporum cells were also characterized by MALDI-MSI at 30 h of incubation (Figure 2 and Supplementary Figure S6).

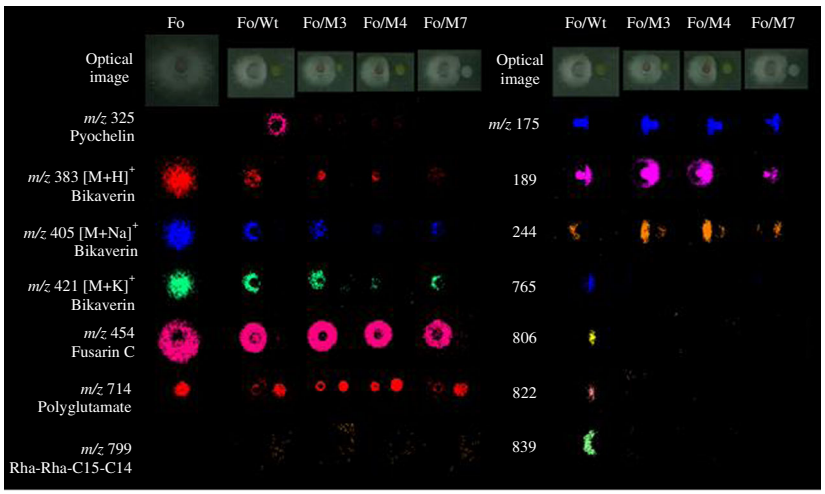

Figure 2. MALDI-MSI of *F. oxysporum* monocultures, and interaction of *B. seminalis* and *F. oxysporum* on PDA medium at 30 h of incubation. Fo = *F. oxysporum*; Wt = wild-type *B. seminalis*; M3/M4/M7 = *B. seminalis* mutants

To better characterize such ions, a *F. oxysporum* extract was also analyzed by ESI-FT-ICR-MS and ESI-Q-TOF-MS. Bikaverin [40] was detected in its protonated (*m/z* 383.0758, Δ = –0.8 ppm), sodiated (*m/z* 405.0578, Δ = – 0.8 ppm), and potassiated (*m/z* 421.0316, Δ = –1.0 ppm) forms (Supplementary Figures S7–S9), whereas fusarin C [41, 42] was detected solely as its sodiated molecule of *m/z* 454.1831 (Δ = –1.1 ppm, Supplementary Figures S7 and S10). Additionally, polyglutamate of *m/z* 714 was also detected in *F. oxysporum* by MALDI-MSI. The reddish pigment bikaverin detected herein for *F. oxysporum* is known to be produced by many *Fusarium* species [43], as well *Mycogone jaapii* [44]. This mycotoxin has been found to display antibiotic activity against oomycete pathogens, plant pathogenic fungi, and protozoa, as well as antitumoral activity against different cancer cell lines [40, 45]. For *F. oxysporum*, therefore, antibiotic effects of bikaverin probably provide advantages to its survival in competitive environments. Fusarin C is also a mycotoxin found in several *Fusarium* species [42, 46, 47], is mutagenic, and its carcinogenic properties represent a potential health risk to humans and animals [47, 48].

The bacterial and fungal strains were also inoculated in a side-by-side interaction on PDA medium, and a significant fungal inhibition in the interaction with wild-type *B. seminalis* TC3.4.2R3 was observed by MALDI-MSI at 30 h. No pyochelin production was detected in all mutants during coculture at 30 h of incubation (Figure 2 and Supplementary Figure S11), suggesting that the *B. seminalis* antagonism results from the antifungal activity of pyochelin, perhaps working in synergy with other unidentified biomolecules, since other diffuse metabolites of unknown identity (*m/z* 275 and 277) were also detected in *B. seminalis*, which varied greatly in the interspecies interactions of the mutants with the *F. oxysporum*. Also, since these mutants are defective in the expression of a glycosyltransferase gene present in the *wcb* cluster, the result suggests that this gene is related to the function of pyochelin cluster, or to the synthesis of synergistic molecules that work with pyochelin in this interaction.

Observing the optical image, there is a similarity in the inhibition effectuated by the M4 mutant strain with the wild-type *B. seminalis* strain (Figure 2), but this similarity was not observed to the molecular level. It is possible that M4 strain produces bioactive molecules that are not detectable by MALDI-MSI. The colony-associated polyglutamate remained unchanged in the interactions, but no Rha-Rha-C15-C14 production was detected. Both bikaverin and fusarin C continued to be produced by *F. oxysporum* during the interactions, but the MALDI-MSI spatial distribution of fusarin C remained unchanged in the coculture of the fungus with the mutants. Interestingly, the interaction zone between wild-type *B. seminalis* and *F. oxysporum* showed additional molecules (*m/z* 175, 189, 244, 765, 806, 822, and 839, Figure 2) produced by the defense mechanisms of either the fungus or the bacterium. Again, to try to better characterize these molecules, inhibition zone extracts were subjected to ESI-FT-ICR-MS, but the trace defense metabolites detected by MALDI-MSI, and likely produced at very low abundances, could not be detected when diluted in the extracts.

Using MALDI-MSI, we found, therefore, that the metabolite pyochelin is used by *B. seminalis* TC3.4.2R3 to inhibit *F. oxysporum* growth, probably in a synergistic action with other diffuse metabolites. The bikaverin and fusarin C mycotoxins were also detected, probably acting as defense molecules of *F. oxysporum* against the bacteria. A better understanding of this chemical interaction mechanism may provide an approach to find new bioactive metabolites. Our preliminary study points to molecules related to the interaction of *B. seminalis* and *F. oxysporum,* which coexist in the sugarcane roots, hence pointing to a potential strategy to biocontrol this phytopathogen, and likely other plant pathogens.

Acknowledgements

The authors gratefully acknowledge financial support from FAPESP – São Paulo Research Foundation, Brazil (grant 2013/24860-9; 2015/11563-1), which enabled the present

research paper. They thank Bruker of Brazil for the software SCiLS Lab, and Professor Anita J. Marsaioli (IQ/Unicamp) for providing the use of the microbiology laboratory.

Compliance with Ethical Standards

Conflict of Interest The authors declare no conflict of interest.

References

1. Braga, R.M., Dourado, M.N., Araújo, W.L.: Microbial interactions: ecology in a molecular perspective. Braz. J. Microbiol. **47S**, 86–98 (2016)
2. Weller, D.M.: Biological control of soil-borne plant pathogens in the rhizosphere with bacteria. Annu. Rev. Phytopathol. **26**, 379–407 (1988)
3. Raaijmakers, J.M., Vlami, M., de Souza, J.T.: Antibiotic production by bacterial biocontrol agents. Antonie van Leeuwenhoek **81**, 537–547 (2002)
4. Haas, D., Défago, G.: Biological control of soil-borne pathogens by fluorescent pseudomonads. Nat. Rev. Microbiol. **3**, 307–319 (2005)
5. Perin, L., Martínes-Aguilar, L., Castro-Gonzáles, R., Estrada-De-Los-Santos, P., Cabellos-Avelar, T., Guedes, H.V., Reis, V.M., Caballero-Mellado, J.: Diazotrophic *Burkholderia* species associated with field-grown maize and sugarcane. Appl. Environ. Microbiol. **72**, 3103–3110 (2006)
6. Vial, L., Groleau, M.C., Dekimpe, V., Déziel, E.: *Burkholderia* diversity and versatility: an inventory of the extracellular products. J. Microbiol. Biotechnol. **17**, 1407–1429 (2007)
7. Araújo, W.L., Creason, A., Mano, E.T., Camargo-Neves, A.A., Minami, S.N., Chang, J., Loper, J.E.: Genome sequencing and transposon mutagenesis of *Burkholderia seminalis* strain TC3.4.2R3 identify genes contributing to suppression of orchid necrosis caused by *B. gladioli*. Mol. Plant-Microbe Interac. **29**, 435–446 (2016)
8. Parke, J.L.: Population dynamics of *Pseudomonas cepacia* in the pea spermosphere in relation to biocontrol of *Pythium*. Phytopathology **80**, 1307–1311 (1990)
9. McLoughlin, T.J., Quinn, J.P., Bettermann, A., Bookland, R.: *Pseudomonas cepacia* suppression of sunflower wilt fungus and role of antifungal compounds in controlling the disease. Appl. Environ. Microbiol. **58**, 1760–1763 (1992)
10. Hebbar, K.P., Davey, A.G., Merrin, J., Dart, P.J.: Rhizobacteria of maize antagonistic to *Fusarium moniliforme*, a soil-borne fungal pathogen: colonization of rhizosphere and roots. Soil Biol. Biochem. **24**, 989–997 (1992)
11. King, E.B., Parke, J.L.: Biocontrol of aphanomyces root rot and *Pythium* damping-off by *Pseudomonas cepacia* AMMD on four pea cultivars. Plant Dis. **77**, 1185–1188 (1993)
12. Arima, K., Imanaka, H., Kousaka, M., Fukuda, A., Tamura, G.: Pyrrolnitrin, a new antibiotic substance, produced by *Pseudomonas*. Agric. Biol. Chem **28**, 575–576 (1964)
13. Cartwright, D.K., Chilton, W.S., Benson, D.M.: Pyrrolnitrin and phenazine production by *Pseudomonas cepacia*, strain 5.5B, a biocontrol agent of *Rhizoctonia solani*. Appl. Microbiol. Biotechnol. **43**, 211–216 (1995)
14. Lee, C.H., Kim, S., Hyun, B., Suh, J.W., Yon, C., Kim, C., Lim, Y., Kim, C.: Cepacidine A, a novel antifungal antibiotic produced by *Pseudomonas cepacia*. I. Taxonomy, production, isolation, and biological activity. J. Antibiot. **47**, 1402–1405 (1994)
15. Kang, Y.W., Carlson, R., Tharpe, W., Schell, M.A.: Characterization of genes involved in biosynthesis of a novel antibiotic from *Burkholderia cepacia* BC11 and their role in biological control of *Rhizoctonia solani*. Appl. Environ. Microbiol. **64**, 3939–3947 (1998)
16. Abdel-Mawgoud, A.M., Lépine, F., Déziel, E.: Rhamnolipids: diversity of structures, microbial origins, and roles. Appl. Microbiol. Biotechnol. **86**, 1323–1336 (2010)
17. Ying, J., Yoshihara, T., Ichihara, A., Ishikuri, S., Uchino, H.: Structural identification of cepaciamide A, a novel fungitoxic compound from *Pseudomonas cepacia* D-202. Tetrahedron Lett. **37**, 1039–1042 (1996)
18. Thomas, M.S.: Iron acquisition mechanisms of the *Burkholderia cepacia* complex. Biometals **20**, 431–452 (2007)
19. Shoji, J., Hinoo, H., Kato, T., Hattori, T., Hirooka, K., Tawara, K.: Isolation of cepafungins I, II, and III from *Pseudomonas* species. J. Antibiot. **43**, 783–787 (1990)
20. Schellenberg, B., Bigler, L., Dudler, R.: Identification of genes involved in the biosynthesis of the cytotoxic compound glidobactin from a soil bacterium. Environ. Microbiol. **9**, 1640–1650 (2007)
21. Kirinuki, T., Ichiba, T., Katayama, K.: General survey of action site of altericidins on metabolism of *Alternaria kikuchiana* and *Ustilago maydis*. J. Pesticide Sci. **9**, 601–610 (1984)
22. Kang, J.G., Shin, S.Y., Kim, M.J., Bajpai, V., Maheshwari, D.K., Kang, S.C.: Isolation and antifungal activities of 2-hydroxymethyl-chroman-4-one produced by *Burkholderia* sp. MSSP. J. Antibiot. **57**, 726–731 (2004)
23. Luvizotto, D.M., Marcon, J., Andreote, F.D., Dini-Andreote, F., Neves, A.A.C., Araújo, W.L., Pizzirani-Kleiner, A.A.: Genetic diversity and plant growth related features of Burkholderia spp. from sugarcane roots. World J. Microbiol. Biotechnol. **26**, 1829–1836 (2010)
24. Yang, Y.L., Xu, Y., Straight, P., Dorrestein, P.C.: Translation metabolic exchange with imaging mass spectrometry. Nat. Chem. Biol. **5**, 885–887 (2009)
25. Moree, W.J., Phelan, V., Wu, C.H., Bandeira, N., Cornett, D.S., Duggan, B.M., Dorrestein, P.C.: Inter-kingdom metabolic transformations captured by microbial imaging mass spectrometry. Proc. Nat. Acad. Sci. **109**, 13811–13816 (2012)
26. Traxler, M.F., Watrous, J.D., Alexandrov, T., Dorrestein, P.C., Kolter, R.: Interspecies interactions stimulate diversification of the Streptomyces coelicolor secreted metabolome. mBio **4**, 459–413 (2013)
27. Cramer, R.A., Byrne, P.F., Brick, M.A., Panella, L., Wickliffe, E., Schwartz, H.F.: Characterization of *Fusarium oxysporum* isolates from common bean and sugar beet using pathogenicity assays and random-amplified polymorphic DNA markers. J. Phytopathol. **151**, 352–360 (2003)
28. O'Donnell, K., Kistler, H.C., Cigelnik, E., Ploetz, R.: Multiple evolutionary origins of the fungus causing Panama disease of banana: concordant evidence from nuclear and mitochondrial gene genealogies. Proc. Nat. Acad. Sci. **95**, 2044–2049 (1998)
29. Diehl, H.C., Beine, B., Elm, J., Ahrens, M., Eisenacher, M., Marcus, K., Meyer, H.E., Henkel, C.: The challenge of on-tissue digestion for MALDI MSI – a comparison of different protocols to improve imaging experiments. Anal. Bioanal. Chem. **407**, 2223–2243 (2015)
30. Coxt, C.D., Rinehart, K.L., Moore, M.L., Cook, J.C.: Pyochelin: novel structure of an iron-chelating growth promoter for *Pseudomonas aeruginosa*. Proc. Nat. Acad. Sci. **78**, 4256–4260 (1981)
31. Funston, S.J., Tsaousi, K., Rudden, M., Smyth, T.J., Stevenson, P.S., Marchant, R., Banat, I.M.: Characterizing rhamnolipid production in *Burkholderia thailandensis* E264, a non-pathogenic producer. Appl. Microbiol. Biotechnol. **100**, 7945–7956 (2016)
32. Pereira, J.F.B., Gudiña, E.J., Dória, M.L., Domingues, M.R., Rodrigues, L.R., Teixeira, J.A., Coutinho, J.A.: Characterization by electrospray ionization and tandem mass spectrometry of rhamnolipids produced by two *Pseudomonas aeruginosa* strains isolated from Brazilian crude oil. Eur. J. Mass Spectrom. **18**, 399–406 (2012)
33. Haubler, S., Nimtz, M., Domke, T., Wray, V., Steinmetz, I.: Purification and characterization of a cytotoxic exolipid of *Burkholderia pseudomallei*. Infect Immun. **66**, 1588–1593 (1998)
34. Al-Tahhan, R.A., Sandrin, T.R., Bodour, A.A., Maier, R.M.: Rhamnolipids-induced removal of lipopolysaccharide from *Pseudomonas aeruginosa*: effect on cell surface properties and interaction with hydrophobic substrates. App. Environ. Microbiol. **66**, 3262–3269 (2000)
35. Dayvey, M.E., Caiazza, N.C., O'Toole, G.A.: Rhamnolipid surfactant production affects biofilm architecture in *Pseudomonas aeruginosa* PAO1. J. Bacteriol. **185**, 1027–1036 (2003)
36. Boles, B.R., Thoendel, M., Singh, P.K.: Rhamnolipids mediate detachment of *Pseudomonas aeruginosa* from biofilms. Mol. Microbiol. **57**, 1210–1223 (2005)
37. Gonzalez, D.J., Xu, Y., Yang, Y.L., Esquenazi, E., Liu, W.T., Edlund, A., Duong, T., Du, L., Molnár, I., Gerwick, W.H., Jensen, P.R., Fishbach, M., Liaw, C.C., Straight, P., Dorrestein, P.C.: Observing the invisible through imaging mass spectrometry, a window into the metabolic exchange patterns of microbes. J. Proteom. **75**, 5069–5076 (2012)
38. Neves, A.A.C.: [Identificação de genes de *Burkholderia* sp. associados a antagonismo a microrganismos fitopatogênicos.] Master thesis in Biotechnology, University of Mogi das Cruzes, Mogi das Cruzes, SP, 62 p. (2011)

39. Burger, M.M., Glaser, L., Burton, R.M.: Formation of rhamnolipids of *Pseudomonas aeruginosa*. Methods Enzymol. **8**, 441–445 (1966)
40. Busman, M., Butchko, R.A.E., Proctor, R.H.: LC-MS/MS method for the determination of the fungal pigment bikaverin in maize kernels as an indicator of ear rot. Food Add. Contam: Part A **29**, 1736–1742 (2012)
41. Kleigrewe, K., Söhnel, A.C., Humpf, H.U.: A new high-performance liquid chromatography-tandem mass spectrometry method based on dispersive solid phase extraction for the determination of the mycotoxin fusarin C in corn ears and processed corn samples. J. Agric. Food Chem. **59**, 10470–10476 (2011)
42. Han, Z., Tangni, E.K., Huybrechts, B., Munaut, F., Scauflaire, J., Wu, A., Callebaut, A.: Screening survey of co-production of fusaric acid, fusarin C, and fumonisins B1, B2, and B3 by *Fusarium* strains grown in maize grains. Mycotoxin Res. **30**, 231–240 (2014)
43. Chelkowski, J., Zajkowski, P., Visconti, A.: Bikaverin production of *Fusarium* species. Mycotoxin Res. **8**, 73–76 (1992)
44. Terashima, N., Ishida, M., Hamasaki, T., Hatsuda, Y.: Isolation of bikaverin from *Mycogone jaapii*. Phytochemistry **11**, 2880 (1972)
45. Limón, M.C., Rodríguez-Ortiz, R., Avalos, J.: Bikaverin production and applications. Appl. Microbiol. Biotechnol. **87**, 21–29 (2010)
46. Barrero, A.F., Sanchez, J.F., Oltra, J.E., Tamayo, N., Cerdá-Olmedo, E., Candau, R., Avalos, J.: Fusarin C and 8Z-fusarin C from *Gibberella fujikuroi*. Phytochemistry **30**, 2259–2263 (1991)
47. Cantalejo, M.J., Torondel, P., Amate, L., Carrasco, J.M., Hernandez, E.: Detection of fusarin C and trichothecenes in *Fusarium* strains from Spain. J. Basic Microbiol. **39**, 43–153 (1999)
48. Sondergaard, T.E., Hansen, F.T., Purup, S., Nielsen, A.K., Bonefeld-Jorgensen, E.C., Giese, H., Sorensen, J.L.: Fusarin C acts like an estrogenic agonist and stimulates breast cancer cells in vitro. Toxicol. Lett. **205**, 116–121 (2011)